DNA Twist Stability Changes with Magnesium(2+) Concentration

Onno D. Broekmans, Graeme A. King, Greg J. Stephens, and Gijs J. L. Wuite*
LaserLaB Amsterdam and Department of Physics and Astronomy VU University Amsterdam, 1081 HV Amsterdam, Netherlands
(Received 14 February 2015; published 21 June 2016)

To understand DNA elasticity at high forces ($F > 30$ pN), its helical nature must be taken into account, as a coupling between twist and stretch. The prevailing model, the wormlike chain, was previously extended to include this twist-stretch coupling. Motivated by DNA's charged nature, and the known effects of ionic charges on its elasticity, we set out to systematically measure the impact of buffer ionic conditions on twist-stretch coupling. After developing a robust fitting approach, we show, using our new data set, that DNA's helical twist is stabilized at high concentrations of the magnesium divalent cation. DNA's persistence length and stretch modulus are, on the other hand, relatively insensitive to the applied range of ionic strengths.

DOI: 10.1103/PhysRevLett.116.258102

Mechanical perturbations of the DNA double helix form a crucial step during many of the cell's life-sustaining processes. When proteins bind, replicate, compact, and repair the genome, the DNA molecule is bent, stretched, and twisted. A detailed understanding of DNA's elastic response to these perturbations is therefore a prerequisite for a deep quantitative insight into the biology of the cell. The single-molecule techniques that have been developed over the past two decades [1,2] have greatly contributed to this understanding: it is now routinely possible to directly manipulate single molecules of DNA, and monitor their response to stretch and twist under a wide variety of experimental conditions. One such technique is the optical tweezers (Fig. 1, schematic), which can be used to accurately measure the force response of DNA [3]. By modeling the corresponding force-extension data, we can then not only improve upon our structural understanding of DNA, but it is also possible to infer the mechanisms of action of DNA-binding proteins from the changes they induce in the data [4,5].

Below mechanical loads of ~30 pN, the force response of double-stranded DNA (dsDNA) is accurately modeled by the extensible wormlike chain (eWLC) [6,7]. This well-established, semiclassical model describes the molecule as simply an isotropic, extensible rod: Entropic bending fluctuations, characterized by a persistence length L_p (50 nm for dsDNA under physiological conditions), and enthalpic stretching of the DNA backbone, characterized by the stretch modulus S (1500 pN [8]), are balanced by the work performed by the stretching force F, leading to a relative extension d/L_c (end-to-end distance over contour length). Beyond 30 pN, however, dsDNA's helical structure needs to be taken into account [8–10]. This introduces an energy cross term between the molecule's twist and stretch degrees of freedom. Only relatively recently, Gross *et al.* found it possible to incorporate this effect into the eWLC, yielding the "twistable wormlike chain" (tWLC) [8]:

$$\frac{d}{L_c} = 1 - \frac{1}{2}\left(\frac{k_B T}{F L_p}\right)^{1/2} + \frac{C}{-g(F)^2 + SC} F, \qquad (1)$$

where C is the molecule's twist rigidity (440 pN nm^2 [8]), and $g(F)$ is the twist-stretch coupling. As illustrated schematically in Fig. 2(a), a positive value of g would correspond to the intuitive case of DNA unwinding as it is being stretched. In reality, DNA slightly *overwinds* up to

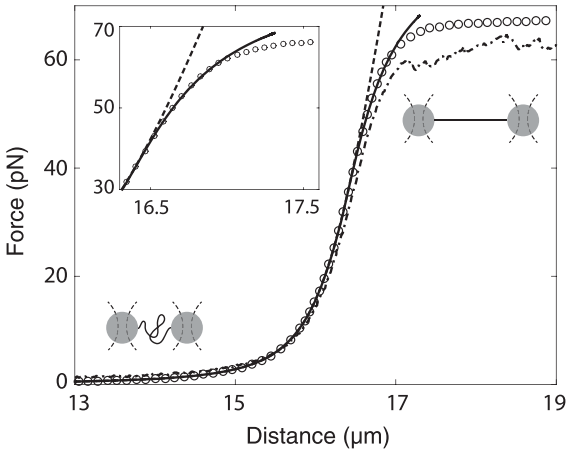

FIG. 1. Typical force-extension data for double-stranded DNA (open circles) stretched using optical tweezers (schematically shown: a DNA molecule is tethered between two microbeads held in optical traps). Whereas the extensible wormlike chain (dashed line) only fits the data for forces up to ~30 pN, the twistable wormlike chain (solid line) expands this range to ~60 pN. Shown is averaged data for buffer conditions (500 mM NaCl, no Mg^{2+}, $N = 151$). For comparison, a single low-salt curve (75 mM NaCl, dash-dotted line) is shown, illustrating the effects of end-unpeeling.

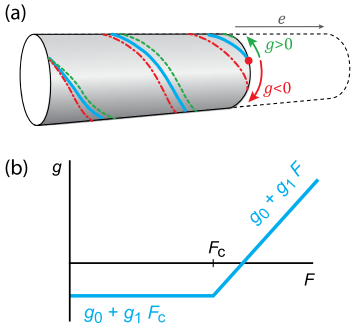

FIG. 2. (a) A "toy model" of DNA twist-stretch coupling, based on [9]. For positive values of the twist-stretch coupling g, the right-handed DNA helix (blue, solid line) would unwind (green, dashed line) when stretched (increasing relative extension e). In reality, for forces up to ~35 pN, DNA *overwinds* when stretched (red, dash-dotted line). (b) The force dependence of the twist-stretch coupling g of dsDNA is modeled in the twistable wormlike chain as a piecewise linear function [8]: constant up to a critical force F_c (30.6 pN); above F_c, a linear approximation $g(F) = g_0 + g_1 F$ is used.

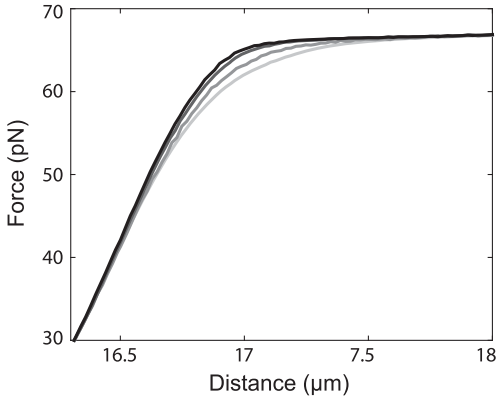

FIG. 3. Double-stranded DNA force-extension data for increasing concentrations of $MgCl_2$ (in a background of 500 mM NaCl and 10 mM TrisHCl, pH 7.6; light to dark: 0, 25, 50, and 100 mM of $MgCl_2$, respectively). For high magnesium concentrations, a clear stiffening of the DNA before the onset of overstretching is observed. Shown is data averaged per magnesium concentration ($N \geq 12$), after correction for systematic measurement errors (see main text).

~35 pN—a finding with major implications for proteins that have to twist DNA upon binding [9,10]. More importantly, g is force dependent: above a critical force F_c of ~31 pN, DNA gradually switches from overwinding to underwinding [8,9]. This is modeled in the tWLC by taking g as a piecewise linear function of the force F [see Fig. 2(b) and Supplemental Material [11]]. The force dependence leads to a marked deviation of the DNA's force-extension behavior from that of the extensible wormlike chain (cf. Fig. 1), until, around 65 pN, the DNA undergoes a structural transition known as overstretching, whereby the molecule suddenly lengthens by ~70% over a narrow force range [8,16–18]. Overall, the tWLC substantially extends the range of forces over which dsDNA force-extension data are understood (see Fig. 1).

More importantly, the tWLC captures DNA twist-stretch coupling as the two parameters g_0 and g_1, which can now be obtained from fits to force-extension data. This opens up the possibility of investigating if, and to what extent, twist-stretch coupling is affected by ionic conditions. DNA is, after all, a highly charged molecule, known to interact strongly with cations through its phosphate backbone and major groove [19,20]. These interactions can lead to softening of DNA [21,22], and, for multivalent cations, to bending [23], and even condensation [24]. In this Letter, we therefore set out to quantify DNA twist-stretch coupling as a function of the concentration of the divalent magnesium cation (Mg^{2+}).

Optical tweezers experiments.—Using optical tweezers, we collected single-molecule force-extension data on dsDNA at varying concentrations of magnesium (0–150 mM $MgCl_2$). In brief, we tethered biotinylated λ-phage DNA ($L_c = 16.5$ μm) between two 3.05 μm streptavidin-coated polystyrene microspheres captured in two optical traps, inside a microfluidic flowcell (for details on the instrument and protocols, please refer to [25]). To suppress unpeeling of the untethered ends of the DNA strands, which causes a signature saw-tooth pattern in the overstretching plateau [8] (see Fig. 1), we worked in a background of 500 mM monovalent salt (NaCl) [18,26]. Below forces of 30 pN, force-extension curves were indistinguishable (data not shown), indicating that the persistence length L_p and stretch modulus S were not affected by the addition of divalent salt. Since the force dependence of twist-stretch coupling only affects dsDNA elasticity significantly above ~45 pN, we instead focused on comparing the data in this high-force regime (Fig. 3). For high concentrations of magnesium, we observed a distinct stiffening of the DNA just before the onset of overstretching. This suggested that twist-stretch coupling was specifically affected.

Data analysis approach.—To quantify the stiffening effect, we fitted the data with the tWLC, Eq. (1). Since previous reports have shown the twist rigidity C to be insensitive to ionic strength [27,28], that leaves the model with four fit parameters: L_p, S, g_0, and g_1. Given this large number of parameters, a solid approach for fitting the data was needed. We would like to highlight three key points in the approach we have developed: (1) fitting with the force as the dependent variable; (2) correcting for systematic measurement errors; and (3) global fitting with shared physical parameters [11].

The first point stems from the observation that, in optical tweezers data, the force signal carries the most significant error (and not the distance, which is precisely controlled). As such, when performing a least-squares fit, the force should be the dependent variable [29]. This implies that the model fitted to our data should be an inversion of Eq. (1),

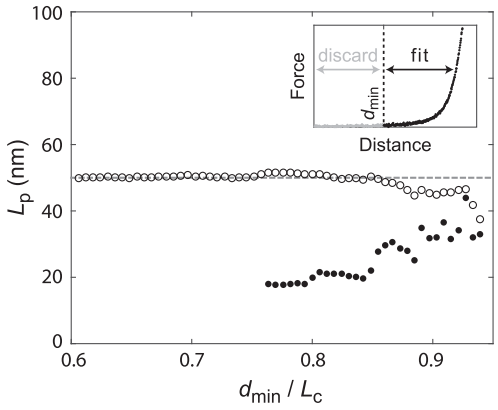

FIG. 4. When fitting optical tweezers force-extension data with the extensible wormlike chain (eWLC) equation as expressed analogously to Eq. (1), with d as the dependent variable, the fit results are highly dependent on the data range used for fitting. As an illustration of this, fragments of simulated data were fitted using nonlinear least squares, using only the data between a distance d_{min} and the eWLC's upper limit of 30 pN (inset). The values found for the persistence length L_p (solid circles) as d_{min} is varied significantly underestimate the actual value (dashed line) and depend strongly on d_{min} (missing points indicate a lack of convergence of the fit). When using an *inverted* version of the eWLC equation, which expresses F as a function of d, a robust and reliable value for L_p is found instead (open circles).

expressing force as a function of distance. The impact of this inversion is illustrated in Fig. 4, for the simplified case of an eWLC fit to simulated data. If Eq. (1) is (incorrectly) used *as is* for the least-squares fit, the value found for L_p changes wildly as more or less data from the low-force tail is included in the fit—in addition to systematically underestimating L_p. When, instead, an inverted version of Eq. (1) is used, the fit result does become reliable, both for L_p and the stretch modulus S (see Supplemental Material [11], Fig. S1) [30].

Second of all, we applied corrections for three systematic measurement errors that are intrinsic to our data: (a) the force at zero extension is not set exactly to zero during each experiment, leading to a random force offset F_0 for each force-extension curve; (b) small variations in microbead diameter lead to a distance offset d_0; and (c) imperfect force sensor calibration causes force data to include a random factor δF. The first two systematic errors were accounted for by including the offsets in the eWLC equation (see Supplemental Material [11]). This amended eWLC equation was fit to the data below 30 pN, and the offsets found were subtracted from the data. The third systematic error was rectified by using the force F_{os} at which the overstretching plateau occurs as a proxy for δF. Within the force resolution of our instrument, there appears to be no correlation between magnesium concentration and F_{os} (see Supplemental Material [11], Fig. S4); we therefore rescaled all force-extension curves to have overlapping overstretching plateaus.

Third, and finally, we opted for a global fitting approach. We grouped all force-extension curves into ensembles by magnesium concentration, implying that the values of the physical parameters (i.e., L_p, S, g_0, and g_1) for curves within each ensemble should be equal. We could thus fit all curves in each ensemble simultaneously, while sharing fit parameters between curves. Fits of simulated data confirmed that, generally, global fitting performs significantly better than individual fitting of the curves, with a decreased sensitivity to the aforementioned systematic measurement errors (see Supplemental Material [11], Figs. S2–S3).

As expected, the tWLC does not fit the full dsDNA force-extension curve up until the overstretching plateau (Fig. 1): the onset of the overstretching phase transition needs to be excluded from the fit. We therefore removed all force-extension data above a maximum force F_{max}, determined by optimizing F_{max} in each magnesium concentration ensemble for a maximum coefficient of determination (R^2) of the fit (see also Supplemental Material [11], Figs. S5–S6). This way, we were able to determine the tWLC fit parameters for each of the measured magnesium concentrations.

Analysis results.—As shown in Fig. 5, the persistence length L_p and the stretch modulus S are stable over the range of magnesium concentrations investigated. This is consistent with the observation that force-extension data below 30 pN (the limit of the eWLC) is equal across magnesium concentrations. Indeed, any electrostatic effects on these parameters are expected to be fully saturated well below the monovalent salt concentration (500 mM NaCl) used in our buffer [21].

The values we find for the persistence length L_p are slightly lower than the widely accepted value of 50 nm at physiological salt concentrations. At buffer conditions more similar to ours, however, previously reported values are consistent [21,22]. Similarly, we measure relatively high values for the stretch modulus S. Both of these results are confirmed, however, using alternative analysis approaches based on the eWLC (see Supplemental Material [11], Fig. S7). Our values for g_0 and g_1 at zero magnesium concentration are statistically indistinguishable from previously reported values [8], and, for low forces, are equivalent to values found in magnetic tweezers studies [9,10].

In contrast to L_p and S, g_1 shows an almost 15% decrease between 0 and 70 mM of magnesium (Fig. 5; see also Supplemental Material [11], Fig. S8, and Fig. S9 for an alternative fitting approach). This can be interpreted as a decreased tendency of the DNA double helix to unwind under high tensile stress—in other words, a stabilization of DNA twist. Qualitatively similar results have been shown before in a bulk study of the relaxation of supercoiled, circular dsDNA by topoisomerase I [31]. There, it was

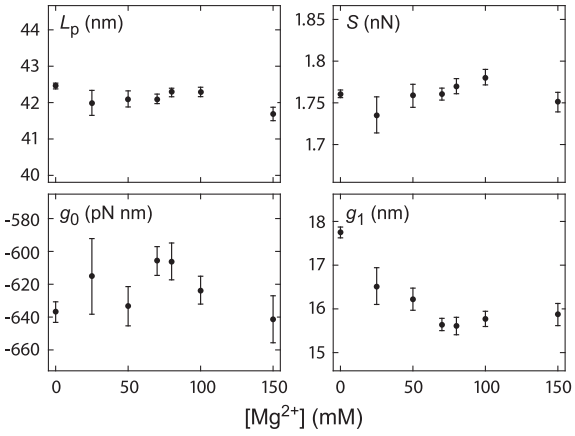

FIG. 5. As the concentration of magnesium$(2+)$ ($MgCl_2$) is increased from 0 to 150 m M (in a background of 500 mM NaCl), the twist-stretch coupling parameter g_1 decreases, indicating a stabilization of dsDNA twist (error bars: bootstrap error, $N \geq 12$). In contrast, the persistence length L_p and stretch modulus S are relatively insensitive to these changes in divalent cation concentration.

speculated that neutralization of the DNA's backbone charge by magnesium$(2+)$ ions diminishes intramolecular repulsion, effectively stabilizing the helical twist of the molecule. The subsequent inversion of the effect at still higher magnesium concentrations is not observed in our study, however. This leaves open the question of the exact molecular mechanism underlying the observed increase of twist stability, and whether the divalent salt homogeneously stabilizes DNA twist, or specifically affects sequence-dependent melting transitions [32]. Future experiments using fluorescent intercalators as reporters of DNA ligation state may help answer these questions.

In conclusion, we have developed a robust analysis approach for force-extension data, based on the twistable wormlike chain model. Our approach gives access to the elasticity regime between 30 and ~60 pN, and thus to information about twist-stretch coupling, directly from stretching data. We have applied this technique to force-extension data of double-stranded DNA at varying concentrations of the magnesium divalent cation ($0-150$ mM, in a background of 500 mM NaCl). The observed stiffening of the DNA at high magnesium concentrations can be interpreted as a nearly 15% decrease of the twist-stretch coupling parameter g_1. DNA's persistence length and stretch modulus, however, remain relatively constant over this concentration range. More generally, we expect our analysis approach to enable expansion of the amount of information that can be extracted from DNA force-extension data, to include a quantification of DNA twist-stretch coupling.

We would like to thank T. T. Perkins for suggesting the initial experiment; M. C. M. de Gunst for useful discussions; and the referees for valuable suggestions. This work has been supported by grants from the Foundation for Fundamental Research on Matter (FOM), which is part of the Netherlands Organization for Scientific Research (NWO), and the European Research Council (starting grant).

Corresponding author.
g.j.l.wuite@vu.nl

[1] S. B. Smith, L. Finzi, and C. Bustamante, Direct mechanical measurements of the elasticity of single DNA molecules by using magnetic beads, Science **258**, 1122 (1992).
[2] M. D. Wang, H. Yin, R. Landick, J. Gelles, and S. M. Block, Stretching DNA with optical tweezers, Biophys. J. **72**, 1335 (1997).
[3] J. R. Moffitt, Y. R. Chemla, S. B. Smith, and C. Bustamante, Recent advances in optical tweezers, Annu. Rev. Biochem. **77**, 205 (2008).
[4] G. Farge, N. Laurens, O. D. Broekmans, S. M. J. L. van den Wildenberg, L. C. M. Dekker, M. Gaspari, C. M. Gustafsson, E. J. G. Peterman, M. Falkenberg, and G. J. L. Wuite, Protein sliding and DNA denaturation are essential for DNA organization by human mitochondrial transcription factor A, Nat. Commun. **3**, 1013 (2012).
[5] I. Heller, T. P. Hoekstra, G. A. King, E. J. G. Peterman, and G. J. L. Wuite, Optical tweezers analysis of DNA-protein complexes, Chem. Rev. **114**, 3087 (2014).
[6] T. Odijk, Stiff chains and filaments under tension, Macromolecules **28**, 7016 (1995).
[7] J. F. Marko and E. D. Siggia, Stretching DNA, Macromolecules **28**, 8759 (1995).
[8] P. Gross, N. Laurens, L. B. Oddershede, U. Bockelmann, E. J. G. Peterman, and G. J. L. Wuite, Quantifying how DNA stretches, melts and changes twist under tension, Nat. Phys. **7**, 731 (2011).
[9] J. Gore, Z. Bryant, M. Nöllmann, M. U. Le, N. R. Cozzarelli, and C. Bustamante, DNA overwinds when stretched, Nature (London) **442**, 836 (2006).
[10] T. Lionnet, S. Joubaud, R. Lavery, D. Bensimon, and V. Croquette, Wringing Out DNA, Phys. Rev. Lett. **96**, 178102 (2006).
[11] See Supplemental Material at http://link.aps.org/supplemental/10.1103/PhysRevLett.116.258102, which includes Refs. [12–15], for more details, raw data, and the code for generating the figures in this Letter.
[12] N. Laurens, R. P. C. Driessen, I. Heller, D. Vorselen, M. C. Noom, F. J. H. Hol, M. F. White, R. T. Dame, and G. J. L. Wuite, Alba shapes the archaeal genome using a delicate balance of bridging and stiffening the DNA, Nat. Commun. **3**, 1328 (2012).
[13] O. D. Broekmans, G. A. King, G. J. Stephens, and G. J. Wuite, Double-stranded DNA force-extension data, as a function of magnesium concentration, http://dx.doi.org/10.6084/m9.figshare.1299526 (2015).
[14] O. D. Broekmans, G. A. King, G. J. Stephens, and G. J. Wuite, FDFIT MATLAB Package., http://dx.doi.org/10.6084/m9.figshare.1306616 (2015).
[15] B. Efron and R. Tibshirani, *An Introduction to the Bootstrap* (Chapman & Hall, New York, 1994).

[16] C. Bustamante, J. F. Marko, E. D. Siggia, and S. Smith, Entropic elasticity of Lambda-phage DNA, Science **265**, 1599 (1994).

[17] J. van Mameren, P. Gross, G. Farge, P. Hooijman, M. Modesti, M. Falkenberg, G. J. L. Wuite, and E. J. G. Peterman, Unraveling the structure of DNA during overstretching by using multicolor, single-molecule fluorescence imaging, Proc. Natl. Acad. Sci. U.S.A. **106**, 18231 (2009).

[18] X. Zhang, H. Chen, S. Le, I. Rouzina, P. S. Doyle, and J. Yan, Revealing the competition between peeled ssDNA, melting bubbles, and S-DNA during DNA overstretching by single-molecule calorimetry, Proc. Natl. Acad. Sci. U.S.A. **110**, 3865 (2013).

[19] T. K. Chiu and R. E. Dickerson, 1 A crystal structures of B-DNA reveal sequence-specific binding and groove-specific bending of DNA by magnesium and calcium, J. Mol. Biol. **301**, 915 (2000).

[20] M. Guéroult, O. Boittin, O. Mauffret, C. Etchebest, and B. Hartmann, Mg^{2+} in the major groove modulates B-DNA structure and dynamics, PLoS One **7**, e41704 (2012).

[21] C. G. Baumann, Ionic effects on the elasticity of single DNA molecules, Proc. Natl. Acad. Sci. U.S.A. **94**, 6185 (1997).

[22] J. R. Wenner, M. C. Williams, I. Rouzina, and V. A. Bloomfield, Salt dependence of the elasticity and overstretching transition of single DNA molecules, Biophys. J. **82**, 3160 (2002).

[23] B. Jerkovic and P. H. Bolton, Magnesium increases the curvature of duplex DNA that contains DA tracts, Biochemistry **40**, 9406 (2001).

[24] B. van den Broek, M. C. Noom, J. van Mameren, C. Battle, F. C. Mackintosh, and G. J. L. Wuite, Visualizing the formation and collapse of DNA toroids, Biophys. J. **98**, 1902 (2010).

[25] A. Candelli, G. J. L. Wuite, and E. J. G. Peterman, Combining optical trapping, fluorescence microscopy and micro-fluidics for single molecule studies of DNA-protein interactions, Phys. Chem. Chem. Phys. **13**, 7263 (2011).

[26] G. A. King, P. Gross, U. Bockelmann, M. Modesti, G. J. L. Wuite, and E. J. G. Peterman, Revealing the competition between peeled ssDNA, melting bubbles, and S-DNA during DNA overstretching using fluorescence microscopy, Proc. Natl. Acad. Sci. U.S.A. **110**, 3859 (2013).

[27] F. Mohammad-Rafiee and R. Golestanian, Electrostatic contribution to twist rigidity of DNA, Phys. Rev. E **69**, 061919 (2004).

[28] F. Mosconi, J. F. Allemand, D. Bensimon, and V. Croquette, Measurement of the Torque on a Single Stretched and Twisted DNA using Magnetic Tweezers, Phys. Rev. Lett. **102**, 078301 (2009).

[29] P. Bevington and D. Robinson, *Data Reduction and Error Analysis for the Physical Sciences*, 3rd ed. (McGraw-Hill, Boston, 2003).

[30] This is a nonissue for magnetic tweezers: distance then carries the most error, and Eq. (1) *can* be used as is.

[31] Y. C. Xu and H. Bremer, Winding of the DNA helix by divalent metal ions, Nucleic Acids Res. **25**, 4067 (1997).

[32] C. Storm and P. C. Nelson, Theory of high-force DNA stretching and overstretching, Phys. Rev. E **67**, 051906 (2003).